

# Finite Element Thermal Analysis of Surface Cold Spots Observed during Infrared Video Imaging of a Moving Hot Steel Strip

by J. B. Wiskel, J. Prescott and H. Henein

Dept. Chem/Mat. Eng., University of Alberta, Edmonton, AB, Canada. T6G 2V4, bwiskel@ualberta.ca

## Abstract

Infrared video imaging, in conjunction with an emissivity probe, was used to quantify the surface temperature of a moving TMCP (thermo mechanical processed) steel strip (skelp) following laminar cooling. Low temperature spikes (or cold spots) were observed on the infrared images and were attributed to the presence of oxides on the strip surface. Finite element thermal modelling of the strip, with different imposed thicknesses of surface oxide, was undertaken. Predicted strip surface temperatures show that the presence of cold spots on the infrared images cannot be attributed to an real temperature, but likely arises from a change in emissivity of the oxide as its undergo a phase transformation from  $\text{Fe}_x\text{O}$  to either  $\text{Fe}_3\text{O}_4$  or  $\text{Fe}_2\text{O}_3$ .

## 1. Introduction

A well-established processing technique for manufacturing steel strip (skelp) with acceptable properties, and at a relatively low cost, is Thermo Mechanical Processing (TMCP). This process includes; a reheat furnace, a hot rolling system and a laminar cooling system for reducing the steel strip temperature from the hot rolling temperature to below the austenite to ferrite transformation temperature. The final microstructure (and hence mechanical properties) of hot rolled steel strip (skelp) depends on the microstructure phase(s) produced during the transformation. Thus, an understanding of the temperature profile of the steel strip along the length of the laminar cooling system is important. However, in many TMCP operations, measuring the strip surface temperature as it moves through the laminar cooling system is difficult. There are many challenges in obtaining accurate temperature readings including; the dynamic nature of the strip (e.g. the strip is moving at relatively high speeds  $\approx 4$  m/s), the presence of water on the surface of the strip and the strip surface condition (e.g. the presence of oxides etc.).

In a previous reported work undertaken by the authors [1], an infrared video camera was used to measure the area temperature profile of a steel strip surface immediately following laminar cooling but before strip upcoiling. Calibration (i.e. determining the effective steel emissivity) of the infrared video camera was achieved using an emissivity probe. The temperature readings obtained from the infrared video images of the strip surface were used for; assessment of temperature uniformity and consistency across the strip, quantification of the heat transfer conditions in the direct water impact zones and subsequent verification of a finite element (FE) thermal model of the strip as it transits the laminar cooling system. For the former, low temperature spikes (hence forth known as cold spots) were observed on the strip. It was unknown whether these cold spots are "real" temperatures arising from the presence of low conductivity surface oxides or an artifact of the infrared imaging temperature analysis (i.e. apparent cold spots are regions exhibiting a different emissivity). To assess the former (i.e. the thermal effect of a surface oxide on surface temperature), a FE thermal analysis of the laminar cooling system, which incorporated the presence of surface oxides of varying thicknesses (0, 100, 200 and 500  $\mu\text{m}$ ), was undertaken. The effect of these different thickness oxides on the presence or absence of cold spots on the strip surface was then ascertained from the predicted temperature data.

## 2. Background

The background section of this paper will summarize the infrared video imaging experiments undertaken on a moving microalloyed steel strip as it transits the laminar cooling system. In addition, a review of the FE thermal model of the strip, incorporating varying thicknesses of oxides on the strip surface, will be undertaken.

### 2.1. Industrial Measurement Setup

A schematic of the laminar cooling system (at the end of the TMCP) illustrating the locations of the infrared video camera, emissivity probe and process pyrometers is shown in figure 1. Water side sprays at discrete locations in the laminar cooling system, and before the upcoiler, are used to remove cooling water retained on the strip. The infrared video camera used in this work was a Mikron M7640. This camera features an 8-14 $\mu\text{m}$  spectral detection band and a 640 x 480 focal plane array microbolometer. Based on the physical location of the camera from the strip, and on the number of pixels in the detector, each pixel recorded by the camera corresponds to a surface area of 3mm x 3mm (on a stationary strip). However, as the strip (during the plant trials) is moving at a significant velocity through the laminar cooling system, the actual area of strip encompassed by each pixel on the detector is a function of the infrared camera

imaging rate (30 Hz) and the speed of the strip. The emissivity measurements were obtained using a Mikron MQ 3600 Quantum II Laser Pyrometer. The focal spot of the probe was positioned to coincide with both the process control pyrometer measurement position at the upcoiler and the infrared video camera field of view. The emissivity probe acquisition rate was approximately 400 ms.

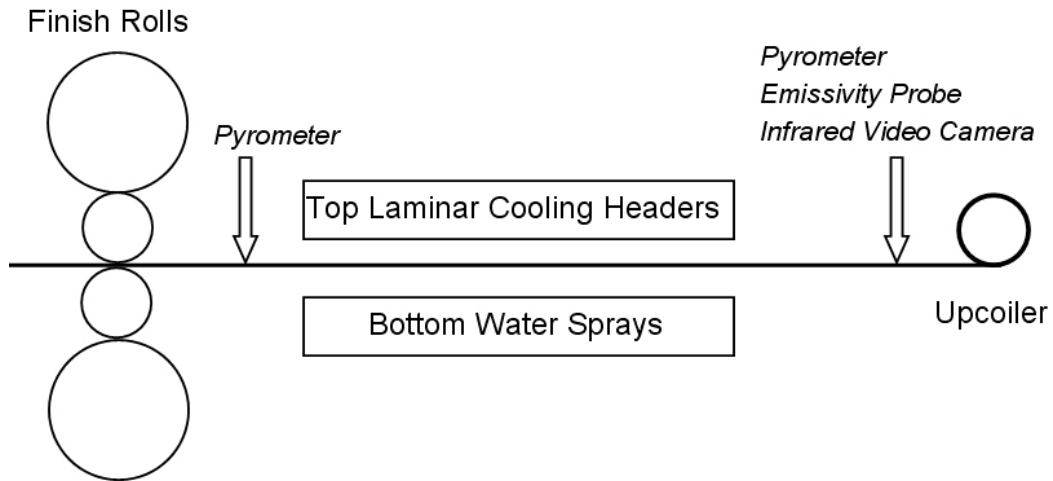


**Fig. 1** Infrared camera, emissivity probe and process pyrometers locations on the laminar cooling system.

## 2.2. FE thermal model

A full description of the FE thermal model is given in reference [1]. The thermal model has been verified for a number of different strips thicknesses and processing conditions. The original model was modified to account for the presence of an oxide layer on the surface of the steel. The mesh used in the FE thermal model simulations is shown in figure 2. Included in this figure is the oxide scale on the strip surface (transparent blue) – for clarity the oxide is not drawn to scale and is only shown schematically. Also included is the thickness ( $\Delta t$ ) of the oxide and the FE model node locations A and B – corresponding to surface temperatures in the model either under the direct water impact (area of the highest heat transfer) or at a surface location remote from the direct water impact (only water boiling heat transfer). The thermophysical properties of the oxide layer include; a temperature dependent thermal conductivity of  $< 6.0 \text{ W/mK}$  (for  $T > 350 \text{ }^\circ\text{C}$ ), a temperature dependent heat capacity (880- 920 J/kg) and a constant density of  $5482 \text{ kg/m}^3$ . The thermal conductivity of the oxide is significantly lower than that of the steel ( $\approx 40 \text{ W/mK}$ ) – it is this large difference in conductivity that may affect surface cooling behaviour. The heat transfer conditions also include radiative cooling after the application of side sprays (i.e. removal of any residual water). The temperature predicted by the FE thermal model at either Node A or Node B will be used to establish the effect of oxide thickness on the surface temperature of the strip at any location along the laminar cooling system including at the infrared camera location (i.e. immediately in front of the upcoiler).

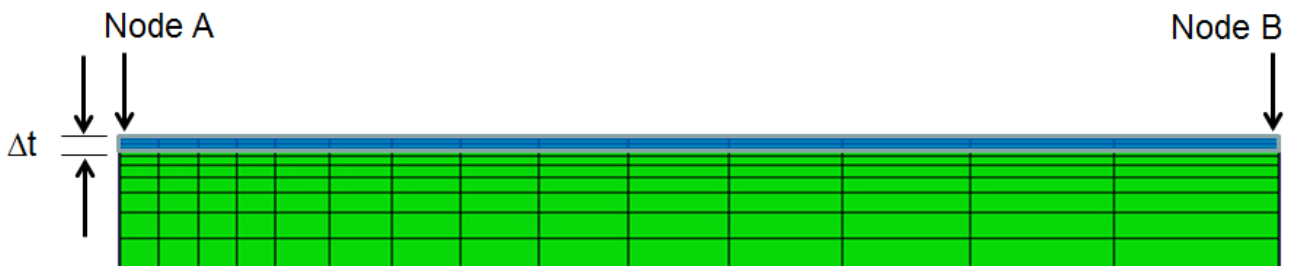


**Fig. 2** Schematic of FE thermal model mesh with oxide surface layer.

### 3. Measurements

This section of the paper presents the emissivity values measured along the length of the strip and the temperature data from a select infrared video image that includes the presence of “cold spots”.

#### 3.1. Emissivity probe data

The emissivity of the steel strip (S475-A12) as a function of time (corresponds to location along the length of the strip) is shown in figure 2. The probe sampling time of  $\approx 400\text{ms}$  corresponds to a physical spacing of emissivity measurements of approximately 2.0 m. As will be subsequently seen, this measurement spacing is much larger than the spacing of the observed cold spots. Also, included in the figure is the normalized strip temperature recorded by the probe. It is observed that the normalized temperature (normalized temperature is the measured temperature divided by a constant temperature value corresponding to the specified coiling temperature) exhibits  $\approx 5$  major spikes (significant reductions) in the measured strip temperature, without a corresponding change in the emissivity. It is not possible to say whether this lack of correlation is real or is related to the operational features of the probe itself. Using the information obtained from figure 2, an emissivity value of 0.94 was used for conversion (within the camera software) of the infrared energy collected by the camera to temperature.

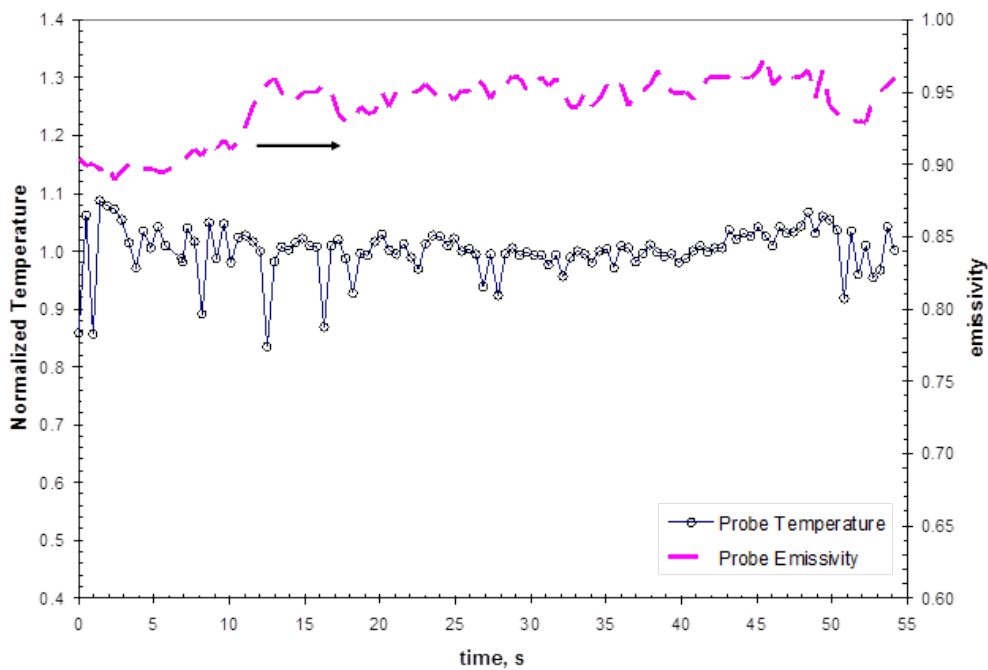


**Fig. 3** Normalized measured temperatures and emissivity value obtained for strip S475-A12.

### 3.2. Infrared Video Temperature Data data

Based on an emissivity of 0.94, the temperature (normalized value) of each individual infrared video image (a 1900 mm long section of strip) was determined. The temperature distribution obtained from a single image from strip S475-A12 is shown in figure 4. The colour contours indicate a relatively uniform strip surface temperature (primarily green) except for the occurrence of light/dark blue regions which indicate a normalized temperature of  $\approx < 0.70$  (i.e. cold spots)

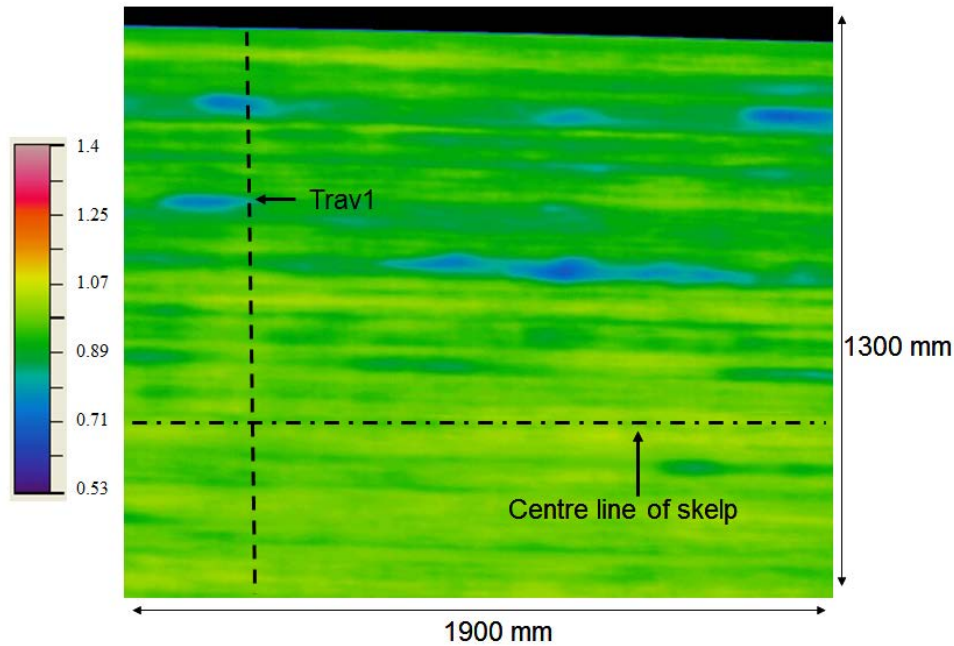


**Fig. 4** Measured normalized temperatures of a single infrared video image from strip S475-A12.

Included in figure 4 is a dashed line traversing the strip width (Trav1). The normalized measured temperatures (at each pixel) along Trav1 are plotted in figure 5. Included in the figure 5 is a vertical arrow indicating the strip centreline and a vertical line corresponding to a change in absolute temperature of 50 °C. The large drop in temperatures occurring at 180 mm and 400 mm correspond to the blue regions observed in figure 4. It is these large decreases in temperature (cold spots) which will be considered in this paper.

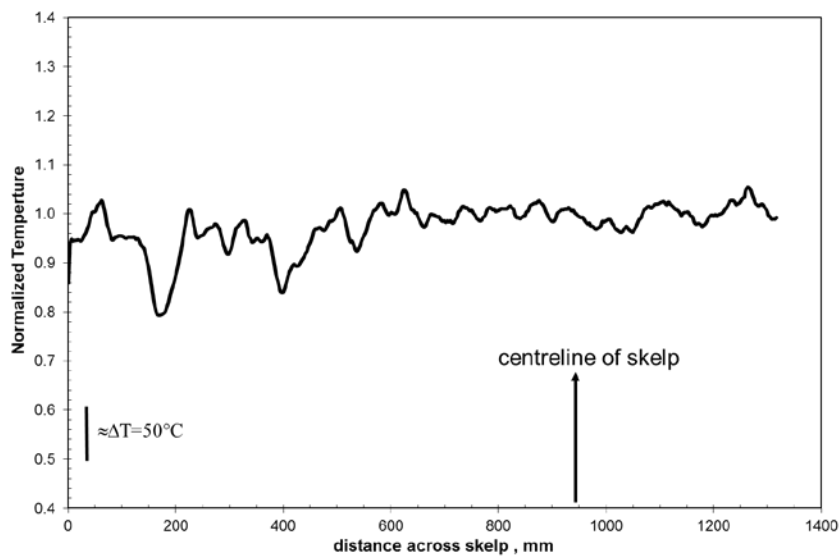


**Fig. 5** Measured normalized strip temperature (vs. distance) along Trav1 from S475-A12.

#### 4. FE model results

As indicated earlier, the thermal model of the strip transiting the laminar cooling system was undertaken with varying oxide thicknesses (i.e.  $\Delta t = 0, 100, 200$  and  $500 \mu\text{m}$ ). The later value is considered a relatively thick oxide. The normalized temperature profile for surface Node A as a function of time in the laminar cooling system for oxide layer thicknesses of  $0 \mu\text{m}$  and  $500 \mu\text{m}$  is shown in figure 6. Included in figure 6 are vertical arrows indicating the location of the upcoiler (i.e. where the infrared measurements were taken) and the minimum surface temperature ( $\approx 495^\circ\text{C}$  for the  $0 \mu\text{m}$  oxide and  $295^\circ\text{C}$  for the  $500 \mu\text{m}$  oxide) predicted. The oscillatory temperatures observed as the strip passes through the laminar cooling system are consistent with either the high rate of heat transfer imparted by direct water impact followed by a rebound in temperature and a more gradual cooling trend as the film boiling is established or the removal of any retained water by the presence of side sprays. Of particular importance for this work is the surface temperature (for both scenarios) at the infrared camera location (i.e. upcoiler). The difference predicted in surface temperature between the  $0 \mu\text{m}$  oxide and  $500 \mu\text{m}$  oxide simulations is only  $3.1^\circ\text{C}$ .

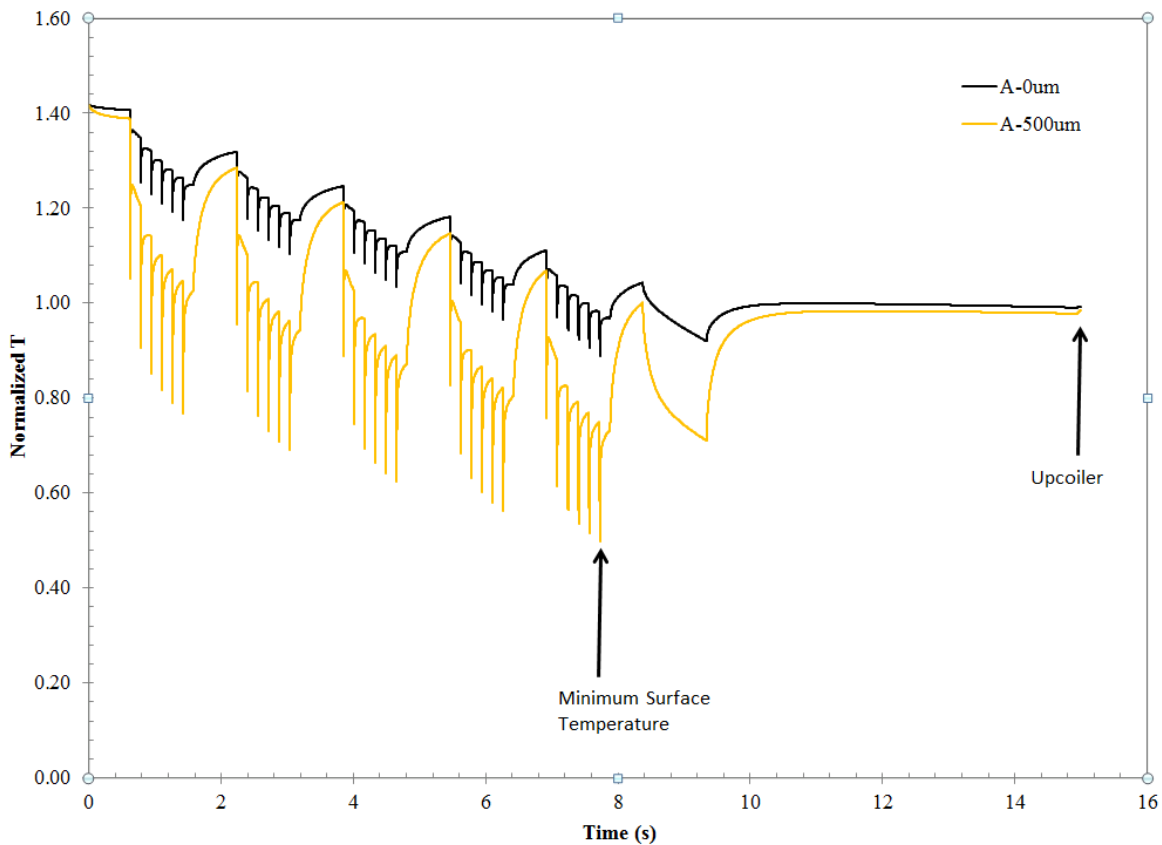


**Fig. 6** Predicted normalized strip temperature at Node A for  $0 \mu\text{m}$  and  $500 \mu\text{m}$  oxide thicknesses

The normalized temperature profile for surface Node B, as a function of time in the laminar cooling system, for oxide layer thickness of  $0 \mu\text{m}$  and  $500 \mu\text{m}$  is shown in figure 7. Included in the figure are vertical arrows indicating the location of the upcoiler (i.e. where the infrared measurements were taken) and the minimum surface temperature ( $538^\circ\text{C}$  for the  $0 \mu\text{m}$  oxide and  $424^\circ\text{C}$  for the  $500 \mu\text{m}$  oxide). Some of the large oscillatory temperatures observed in figure 5 are not present at this surface location on the strip as it is situated at a midpoint between the direct impact water zones. The temperature difference predicted at the upcoiler between the between the  $0 \mu\text{m}$  oxide and  $500 \mu\text{m}$  oxide simulations is only  $2.2^\circ\text{C}$ .

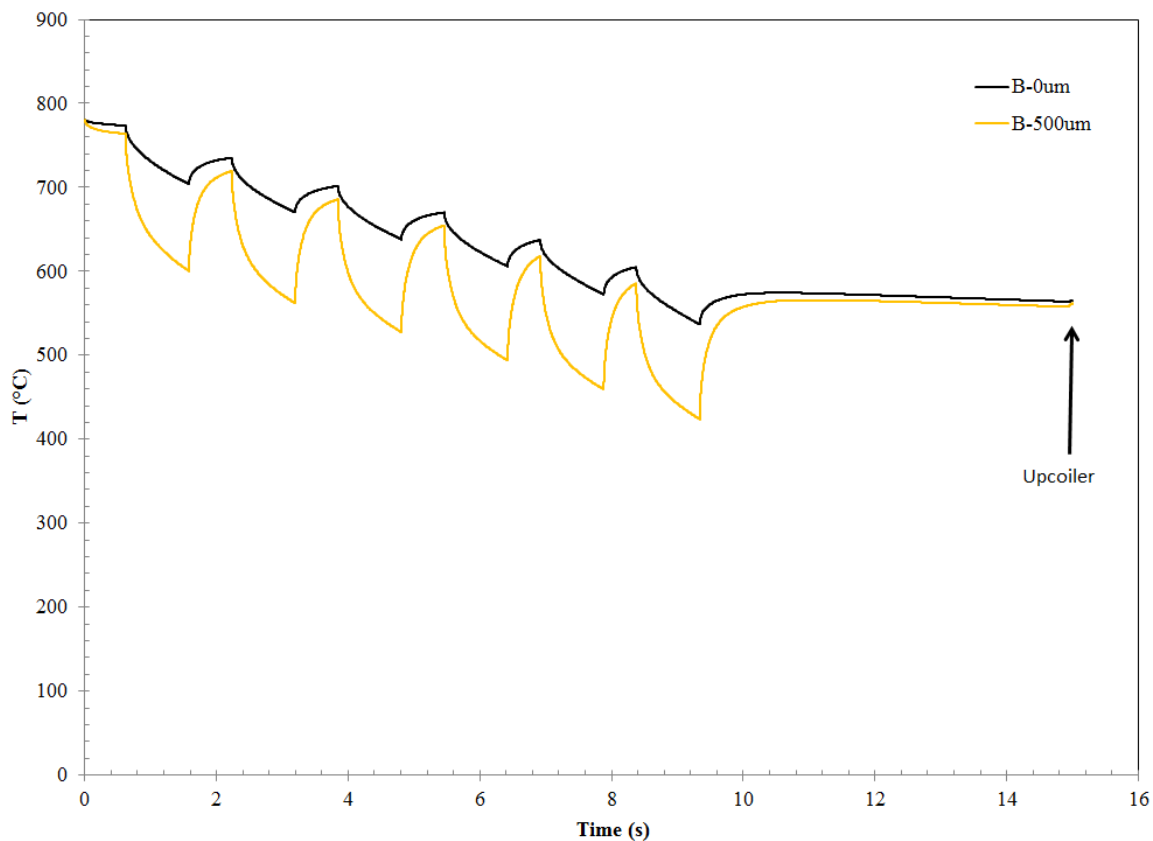


Fig. 7 Predicted normalized strip temperature at Node B for 0 μm and 500 μm oxide thicknesses

## 5. Discussion

The surface temperatures predicted at the upcoiler location (for all the simulated oxide thicknesses) were within 3.1 °C of each other. The large temperature variations observed in figure 2 (between regions of oxide or lack of presence of oxide could not be replicated with the FE thermal model). Thus, it is concluded that the physical presence of oxides (of varying thicknesses) have only a minor effect on localized temperature variation when their temperature is observed at the end of the laminar cooling system (figure 1). However, the surface temperatures predicted along the length of the laminar cooling system (from finish rolls to the infrared camera location), were observed to vary significantly depending upon the simulated oxide thickness (i.e. 0, 100, 200 and 500 μm) being modeled. In particular, the surface temperature for the 500 μm thick surface oxide simulation was predicted to cool to minimum value of 280°C. In comparison, the minimum surface predicted for the 0 μm thick oxide simulation was only 495°C. It should be noted that though the surface temperature was significantly lower for the 500 μm thick oxide simulation (a direct result of the lower thermal conductivity of the oxide), the temperature of the steel below the oxide actually undergoes a more uniform cooling profile than would occur without the presence of the surface oxide.

Previous work [2-5] on the oxidation of steel has indicated that the type of surface oxide present (i.e.  $Fe_xO$ ,  $Fe_3O_4$  and  $Fe_2O_3$ ) present on the strip surface depends on many factors including oxygen content, temperature and cooling rate. The Fe-O equilibrium diagram [6] indicates that below 575°C, the high temperature  $Fe_xO$  phase (Wustite) becomes thermodynamically unstable. The FE thermal modelling work undertaken in this study shows that undercooling below 575 °C (i.e. the driving force for the transformation of  $Fe_xO$  to a more stable oxide state) is a function of oxide thickness. With increased surface oxide thickness, a larger undercooling (e.g. 295 °C for a 500 μm oxide) was observed. Thus, it can be suggested that the cold spots seen in the infrared images result from a variation in local emissivity that arises from a change in the oxide structure (e.g. going from  $Fe_xO$  to either  $Fe_3O_4$  (Magnetite) or  $Fe_2O_3$  (Hematite [7]) due to the variation in thermal behaviour along the length of the laminar cooling system associated with the presence of the oxides.

For the 8-14  $\mu\text{m}$  spectral detection band used in the infrared video camera the change in emissivity that would account for the ( $\approx 75\text{-}100^\circ\text{C}$ ) temperature drop at the cold spots can be approximated [8] by:

$$\frac{\Delta T}{T} = \frac{\lambda}{5 \cdot \lambda_{\max}} \cdot \frac{\Delta \varepsilon}{\varepsilon} \quad (1)$$

where  $\Delta T$  is the change in calculated temperature for a given change in emissivity ( $\Delta \varepsilon$ ). Assuming the peak wavelength  $\lambda_{\max}$  is 3.32  $\mu\text{m}$  (at  $600^\circ\text{C}$ ) and the effective wavelength used for the measurement  $\lambda$  is 11  $\mu\text{m}$ , then for a  $\Delta T = -100^\circ\text{C}$  the value of  $\Delta \varepsilon = -0.24$  or an emissivity of 0.70. Data on the emissivity of different oxide phases (particularly at the temperature of the strip at the upcoiler) was not available in the literature. However, Sprague et al. [9], reported, in the wavelength range of 8-14  $\mu\text{m}$ , that the spectral emissivity of hematite ( $\text{Fe}_2\text{O}_3$ ) can range from 0.76 to 0.97. Similarly, del Campo et al. [7] measured an emissivity's in the range from 0.72 to 0.90 (for a wavelength 8-12  $\mu\text{m}$ ) at  $480^\circ\text{C}$  for an oxidizing steel.

Based on this analysis provided in this paper, it is hypothesized that the presence of the cold spots observed in figure 2 are indirectly indicative of the presence of relatively thick surface oxides via a significant undercooling of the surface and the subsequent transformation of the surface oxide to a lower temperature stable phase. Based on this analysis, an infrared video system may be used indirectly to assess the prevalence these surface oxides and ultimately, to quantify the effectiveness of upstream descaling operations. However, further study of this interrelationship between observed infrared temperature variation and oxide type and thickness and emissivity is needed.

## 6. Conclusions

- 1] Finite element thermal modelling has shown that, from a thermal perspective, the cold spots (large drops in temperature) observed on infrared video images of a moving steel strip (for the laminar cooling system analyzed) are not real.
- 2] The presence of a relatively thick oxide (e.g. 500  $\mu\text{m}$ ) on the strip surface resulted in significant surface undercooling the strips transit the laminar cooling system. This significant undercooling (below the Wustite transformation temperature) may result in the transformation of the surface oxide to either magnetite or hematite with an accompanying change in emissivity.
- 3] The presence of cold spots on an infrared image taken at the upcoiler location are indirectly related to the thickness of the oxide and hence maybe used to assess the effectiveness of upstream strip descaling operations.

## 7. Acknowledgements

The authors would like to thank EVRAZ N.A. Inc. for allowing access to their plant. We would also like to thank NSERC and EVRAZ N.A. for financial support and L. Collins of EVRAZ N.A. for facilitating this work.

## 8. References

- [1] J.B. Wiskel, H. Deng, C. Jefferies and H. Henein, "Infrared Thermography of a TMCP Microalloyed Steel Skelp at the Upcoiler and Its Application in Quantifying the Laminar Jet/Skelp Interaction", *Ironmaking and Steelmaking*, Vol. 38,1, , pp. 35-44, 2011.
- [2] H. Abuluwefa, J.H. Root, R.I.L. Guthrie and F. Ajersch, "Real-Time Observations of the Oxidation of Mild Steel at High Temperature by Neutron Diffraction", *Met. Trans. A*, Vol. 27B, pp. 993- 997, 1996,
- [3] W. Sun, A.K. Tieu, Z. Jiang and C. Lu, High Temperature Oxide Scale Characteristics of Low Carbon Steel in Hot Rolling", *J. Mat. Proc. Tech.*, 155-156, pp. 1307-1312, 2004.
- [4] A.Dey, T. Bhattacharyya and S. Dhara, "Characterization of Hot Rolled Scales – Root Cause Identification and Remedial Action", *Eng. Failure Anal.*, 34, pp. 478-487, 2013.
- [5] R.Y. Chen and W.Y.D. Yuen, "Examination of Oxides Scales of Hot Rolled Steel Products", *ISIJ*, 45, pp. 52-59, 2005
- [6] D. Geneve, D. Rouxel, P. Pigeat, B. Weber and M. Confente, "Surface Composition Modification of High-Carbon Low-Alloy Steels Oxidized at High Temperature in Air", *Appl. Sur. Sci*, 254, pp. 5348-5358, 2008.
- [7] L. delCampo, R.B. Perez-Saez and M.J. Tello, "Iron Oxidation Kinetics Study By Using Infrared Spectral Emissivity Measurements below  $570^\circ\text{C}$ ", *Corr. Sci.*, 50, pp. 194-199, 2008.
- [8] R.F. Leftwich, *Theory and Practice of Radiation Thermometry*, eds. D.P. DeWitt and G. Nutter, John Wiley and Sons, New York, 1988, p502.
- [9] A.L. Sprague, T.L. Roush, R.T. Downs and K. Righter, Response to Comment on Comparison of Laboratory Emission Spectra with Mercury Telescopic Data", *ICARUS*, 143, pp. 409-411, 2000.